ADVANCEMENTS IN STEEL FOR WEIGHT REDUCTION OF P900 ARMOR PLATE

R. A. Howell*, J. S. Montgomery
Survivability Materials Branch
Army Research Lab
Aberdeen Proving Grounds, MD 21001

D.C. Van Aken
Missouri University for Science and Technology
Rolla, MO 65401

ABSTRACT

Ballistic tests were conducted on a high manganese and high aluminum austenitic steel that is age hardenable. These lightweight steels (12 to 18% lower in density) were investigated as alternatives to MIL-PRF-32269 steel alloys for application in P900 perforated armor currently used for Army ground combat systems. Two steel plates with nominal composition in weight percent of Fe-30Mn-9Al-1Si-0.9C-0.5Mo were evaluated for V_{50} against 0.30 caliber armor piercing and 0.50 caliber fragmentation simulation projectiles. At equivalent areal densities to current steels, both plates surpassed the required 0.30 caliber acceptance criteria by 188 and 151 ft/s. Against the 0.50 caliber fragmentation projectile, the calcium treated plate exceeded the MIL-A-46100 V_{50} by 225 ft/s, but the non calcium treated plate underperformed by 39 ft/s.

1. INTRODUCTION

P900 was originally designed in the late 1980's as appliqué armor to counter Soviet small-arms threats (Gooch, 1991). The thin-ribbed section design (see Figure 1) localizes deformation that allow for multi-hit capability. The original P900 was cast from low alloy steels using the lost foam process without regard to material properties. Computer modeling with a re-evaluation of material property requirements and validated by ballistic testing has led to the adaptation of P900 as an armor enhancement in current applications. A quenched and tempered martensitic steel (in accordance with alloy tolerances of MIL-A-46100) met the required hardness and ballistic standards. Expanded metal processes and offset punched plates offer alternative designs to P900, but these solutions do not achieve P900's performance and higher ballistic success rate as measured by MIL-PRF-32269.

Second generation advanced high strength steels that are being developed (Frommeyer, 2006) as lightweight steels for the automotive industry are potential candidates for the P900 armor application. These steels contain high levels of aluminum, which can lower the density by 12 to 18% relative to mild steel. These steels, which are referred to as FeMnAlC, are austenitic and age hardenable by the addition of carbon. Tensile strengths greater than 140 ksi, and elongation to fracture that is greater than 15%, are comparable to quench and tempered low alloy steels currently used. These lightweight steels also have good casting characteristics (high fluidity and low melting temperature) that are as good as ductile iron (Howell et al., 2008). FeMnAlC alloys do not require high cost alloys, such as nickel, cobalt, or chromium and are less costly than titanium alloys. Tailorable properties via age hardening coupled with a 12 to 18% reduced density offer a higher specific strength over quench and tempered steel. Challenges still lie in developing these FeMnAlC alloys to reduce weight without sacrificing P900 armor performance.

2. EXPERIMENTAL PROCEDURE

Two ballistic test plates were cast in a nominal Fe-30Mn-9AL-1Si-0.9C-0.5Mo chemistry. All chemistries are in weight percent. Foundry grade alloys were melted in an induction furnace under argon cover. Horizontal plate molds were prepared from phenolic no-bake (PUNB) olivine sand in lieu of silica sand to prevent reaction of the manganese with the silica sand. One plate measured 12 inch by 18 inch by 0.6 inch, was calcium treated, and utilized electrolytic manganese. The second plate measured 12 inch by 12 inch by 0.72 inch, was not calcium treated, and employed ferromanganese. Post casting, both plates were vacuum solution treated at 1050°C, gas quenched, and aged for 15 hours at 530°C. The non-calcium treated plate was cast at 0.72 inch and subsequently machined to 0.625 inch thickness after solution treatment.

Ballistic testing was performed for V_{50} evaluation of 0.30 caliber armor piercing (AP) and 0.50 caliber fragmentation simulation projectiles (FSP) at 0° obliquity. The FeMnAlC ballistic results were compared on an areal density equivalency to the MIL-PRF-32269

Report Documentation Page

1. REPORT DATE	2. REPORT TYPE	3. DATES COVERED
DEC 2008	**N/A**	**-**

4. TITLE AND SUBTITLE	5a. CONTRACT NUMBER
Advancements In Steel For Weight Reduction Of P900 Armor Plate	5b. GRANT NUMBER
	5c. PROGRAM ELEMENT NUMBER

6. AUTHOR(S)	5d. PROJECT NUMBER
	5e. TASK NUMBER
	5f. WORK UNIT NUMBER

7. PERFORMING ORGANIZATION NAME(S) AND ADDRESS(ES)	8. PERFORMING ORGANIZATION REPORT NUMBER
Survivability Materials Branch Army Research Lab Aberdeen Proving Grounds, MD 21001	

9. SPONSORING/MONITORING AGENCY NAME(S) AND ADDRESS(ES)	10. SPONSOR/MONITOR'S ACRONYM(S)
	11. SPONSOR/MONITOR'S REPORT NUMBER(S)

12. DISTRIBUTION/AVAILABILITY STATEMENT
Approved for public release, distribution unlimited

13. SUPPLEMENTARY NOTES
See also ADM002187. Proceedings of the Army Science Conference (26th) Held in Orlando, Florida on 1-4 December 2008, The original document contains color images.

14. ABSTRACT

15. SUBJECT TERMS

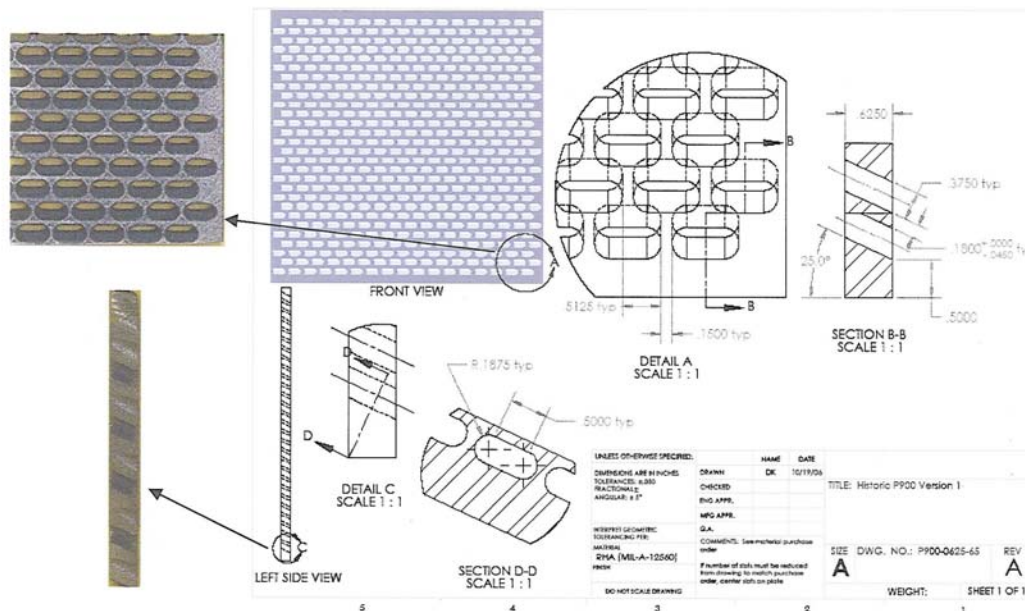| 16. SECURITY CLASSIFICATION OF:			17. LIMITATION OF ABSTRACT	18. NUMBER OF PAGES	19a. NAME OF RESPONSIBLE PERSON
a. REPORT **unclassified**	b. ABSTRACT **unclassified**	c. THIS PAGE **unclassified**	**UU**	**7**	

Figure 1. Shown above is the 2-D dimensional specification drawing and image of cast P900 armor plate.

acceptance criteria for the 0.30 caliber AP and to MIL-A-46100 steel for the 0.50 caliber FSP requirements. The FSP testing is not called for in the MIL-PRF-32269, but there is no historical FSP data on FeMnAlC alloys. FSP test data was compared to MIL-A-46100 (high hard steel) due to its use in MIL-PRF-32269 as a class 1 material and because of a large historical performance database against the 0.50 caliber FSP.

Charpy impact specimens were machined from each FeMnAlC alloy plate, and tests were performed at room temperature and -40°F. Post fracture analysis of ballistic and Charpy impact tests were performed using optical microscopy and scanning electron microscopy (SEM). An ASPEX-PICA 1020 analytical SEM was used to quantify material cleanliness and perform chemical analysis on both fracture surfaces and metallographically prepared specimens. Wet chemical analysis was also performed on each cast alloy plate. A standardless chemical analysis was also performed using energy dispersive x-ray spectrometry (EDS). Computer aided analytic software quantified primary phase constitution, inclusion chemical content, and inclusion size distribution.

4. RESULTS

The MIL-PRF-32269 cast armor material is designated class 2 and has an acceptance range of 302-352 brinnell hardness number (BHN). The calcium treated plate's hardness measured 351 BHN, and the non-calcium treated plate exceeded the hardness range at 364 BHN. Chemical analysis of each plate is shown

in Table 1. Areal density of each plate was measured to be 35.5 pounds per square foot per inch of thickness (PSF), which is 13% less than rolled homogenous armor (40.8 PSF). The equivalent areal density thickness was 0.525 inch for the calcium treated plate and 0.544 inch for the non calcium treated plate. The 0.30 caliber AP V_{50} of the calcium treated plate exceeded the acceptance criteria by 188 ft/s, and the non treated plate exceeded its equivalent thickness value by 151 ft/s. The 0.50 caliber FSP V_{50} for of the calcium treated plate exceeded MIL-A-46100 by 172 ft/s, but the non calcium treated plate was lower by 39 ft/s.

Figure 2 shows the impact and exit sides of both plates for the 0.30 caliber AP testing. The region of deformation on the impact face is more visible on the non calcium treated specimen that was machined. Visible deformation extends 0.5 inch from the center of impact on both plates. Cracking and pedal formation are observed on the exit side of each plate. Figure 3 shows the impact and exit sides for the 0.50 caliber FSP testing. The visible deformation on the impact side of the non calcium treated plate measured approximately 1.25 inch across the surface. Ductile deformation and cracking are observed on the exit side of both plates. Failure occurred by plugging.

Plug formation occurred by adiabatic shear band formation and subsequent cracking. Metallograpic examination of the plug formation is shown in Figure 4. Both plates had a dendritic austenite microstructure with 5 volume % ferrite. Figure 4(b) shows clearly the dendrite cast structure and adiabatic shear between the

porosity and a crack tip near the exit side of the calcium treated plate.
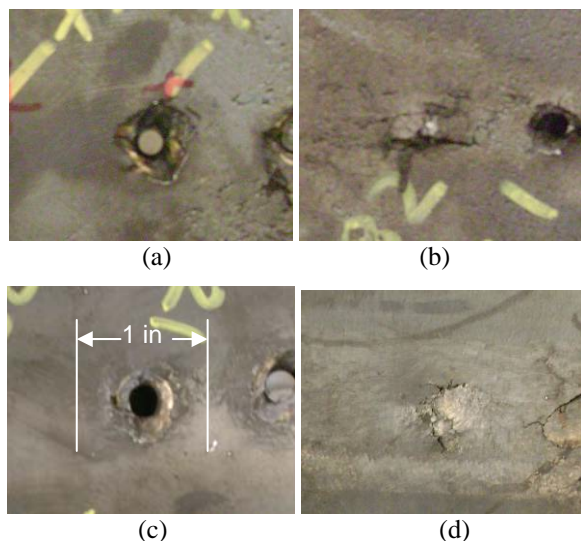

Figure 2. The calcium treated plate shown with 0.30 caliber AP projectile lodged in the plate (a) and resulting combination of ductile deformation and cracking on the exit face (b). The non calcium treated plate shown with dimensional marker illustrating the deformation region on the strike face (c), and the exit side shows ductile deformation and cracking (d).
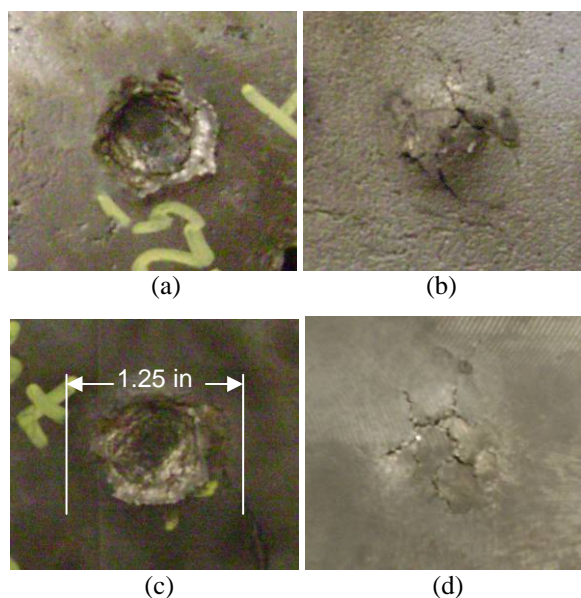

Figure 3. The calcium treated plate is shown with an impact crater from 0.50 caliber FSP (a) and resulting ductile deformation and cracking on the exit face (b). The untreated plate is shown with dimensional marker illustrating the visible deformation on the strike face (c) and the exit side showing ductile deformation and cracking (d).
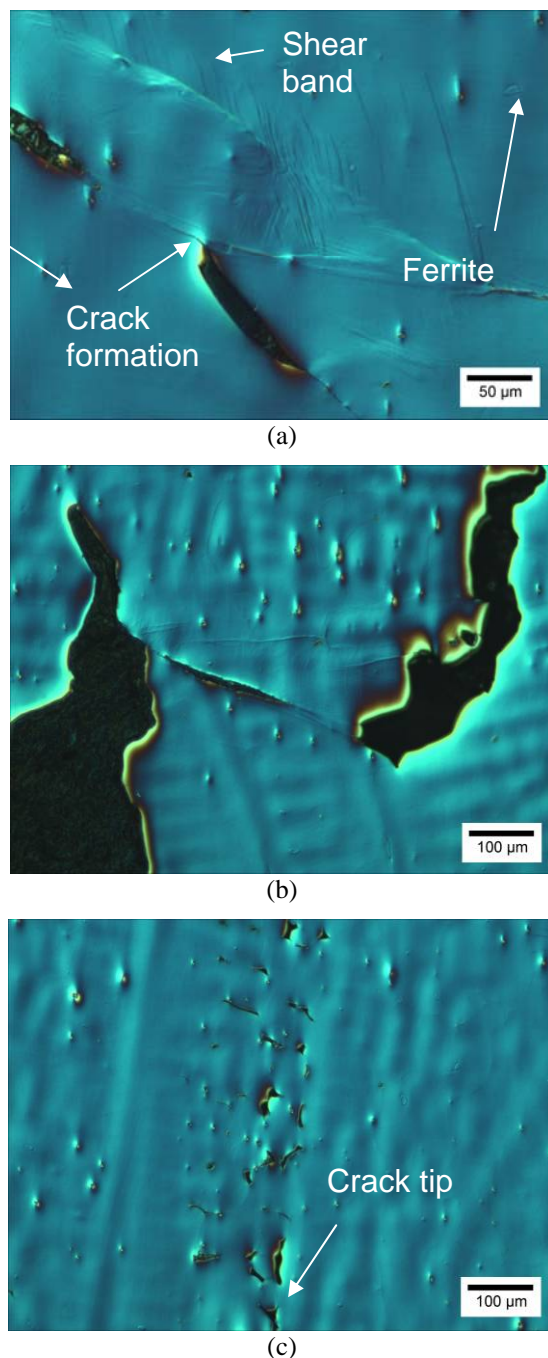

Figure 4. Adiabatic shear band and crack formation is highlighted in (a). Adiabatic shear bands and crack formation occurred between a larger crack tip and porosity near the exit face shown in (b). A large region of defects is observed next to a crack tip in (c).

A crack tip is seen in Figure 4(c) nucleated from a concentration of nonmetallic inclusions. Figure 5 is a pair of EDS generated ternary phase diagrams of this field showing that the inclusions are sulfides and oxides of high manganese concentration.

TABLE 1. Chemical Content of Tested Alloys

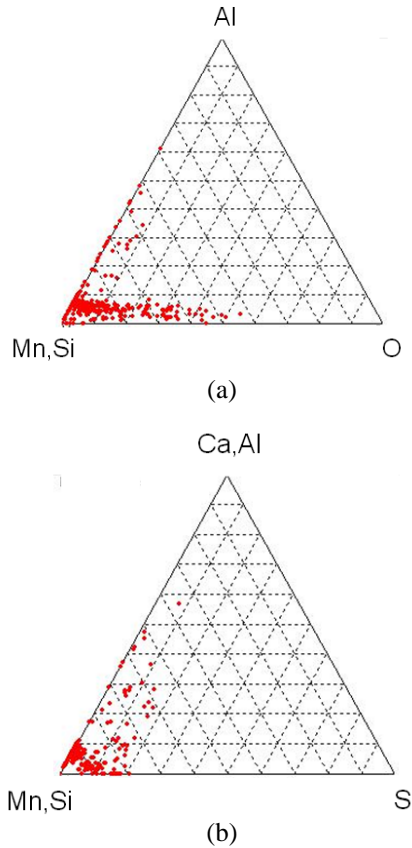| Plate	Fe	Mn	Al	Si	C	Mo	S	P
Calcium Treated	Bal	30.21	8.85	1.01	0.89	0.31	0.0008	0.006
Non-calcium Treated	Bal	29.07	8.28	0.92	0.94	0.33	0.006	0.043

(a)

(b)

Figure 5. Chemical mapping of nonmetallic inclusions on ternary phase diagrams were made by an EDS mapping of the defect field shown in Figure 4(c). The primary oxygen inclusion chemistries included manganese, silicon, and aluminum (a) with predominately manganese sulfides (b).

Charpy impact energy for the calcium treated plate was 54 ft-lbs at room temperature and 10 ft-lbs at -40°F. The impact energy of the non calcium treated plate was much lower at values of 10 ft-lbs at room temperature and 7 ft-lbs at -40°F. An interdendritic fracture was observed for both materials (see Figure 6). As an aid to the reader a graphical representation of the dendrite is superposed on Figure 6. An EDS scan of the fracture surface (see Figure 7) shows higher amounts of sulfur and phosphorous on the non-calcium treated alloy. The elemental sulfur map shows regions of high concentration on the non calcium treated material. The higher levels of phosphorous and sulfer are corroborated by the wet chemical analysis shown in Table 1. The non calcium treated plate has a sulfur content at 0.06 % and

phosphorous content at 0.043 %. The calcium treated plate was lower in both phosphorous and sulfur with levels of 0.006% and 0.0008%, respectively. A side-by-side comparison of metallographic specimens from the Charpy bars is shown in Figure 8. Both microstructures are primary austenite with less than 5% by volume ferrite. The dendrite arm spacing in the calcium treated plate measured 81 μm and 42 μm in the non calcium treated plate. A greater density of nonmetallic inclusions is visible in the non calcium treated plate.
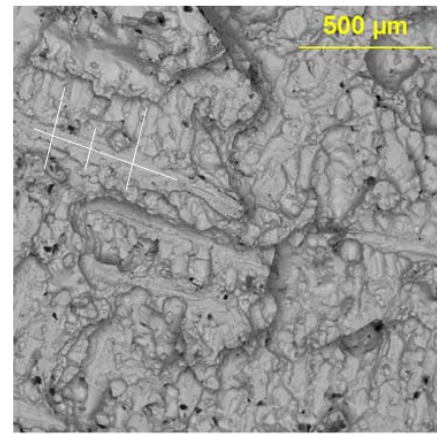
(a)
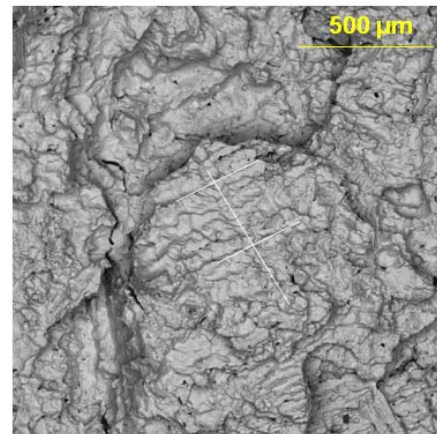
(b)

Figure 6. Back scattered electron images of Charpy bar fracture surfaces from the calcium treated plate (a) and non calcium treated (b). Charpy specimens were cut from solid plate and machined after ageing. The intergranular dendritic fracture pattern is made evident in both images by a skeletal outline. Crack formation is observed in the non calcium treated alloy (b).
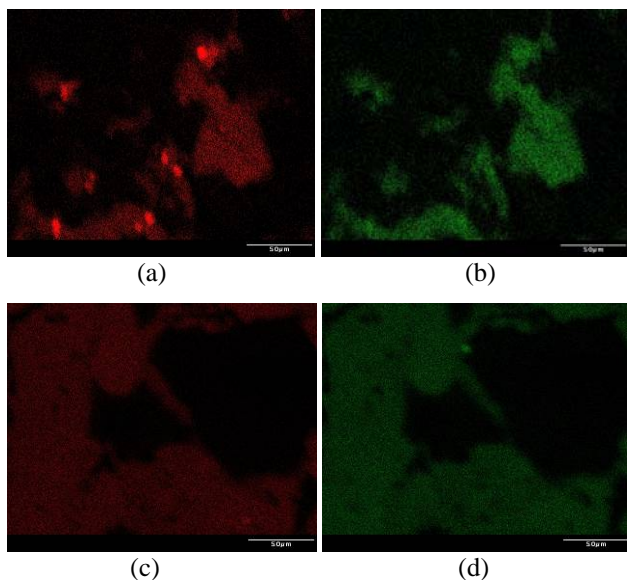
(a)

(b)

(c)

(d)

Figure 7. Elemental (EDS) mapping of fracture surface scans show higher concentrations of sulfur (a) and phosphorous (b) on the non calcium treated material as compared to the calcium treated alloy for sulfur (c) and phosphorous (d).

The ASPEX-PICA 1020 inclusion mapping software was used to compare both steels. Chemistry mapping results are shown in Figure 9 and a histogram of inclusion size comparison is shown in Figure 10 for equivalent test areas. Inclusion chemistry for each steel are comparable; however, the calcium treated steel is much cleaner, i.e. a lower inclusion count. The untreated plate has a greater number of inclusions by a ratio greater than 2:1 in each of the size categories.

5. DISCUSSION

The Fe-30Mn-9Al-1Si-0.9C-0.5Mo alloys meet MIL-PRF-322269 0.30 caliber AP acceptance criteria on an equivalent areal density basis. As measured against high hard steel, only the calcium treated steel met expectations with respect to the 0.50 caliber FSP threat. The 0.50 caliber FSP test shows a greater V_{50} separation between the two test pieces. Even though the calcium treated plate was thinner by 0.020 inches, its V_{50} exceeded that of the untreated plate by 211 ft/s.

The non calcium treated plate had lower Charp impact energy than the calcium treated plate at room temperature and at -40°F. Figure 6 shows that both materials fractured interdendritically. The microstructure of both plates appears identical (primary austenite and less than 5% by volume ferrite).

The most dramatic difference between the two cast steels is shown in Table 1 by comparing the phosphorous and sulfur contents.
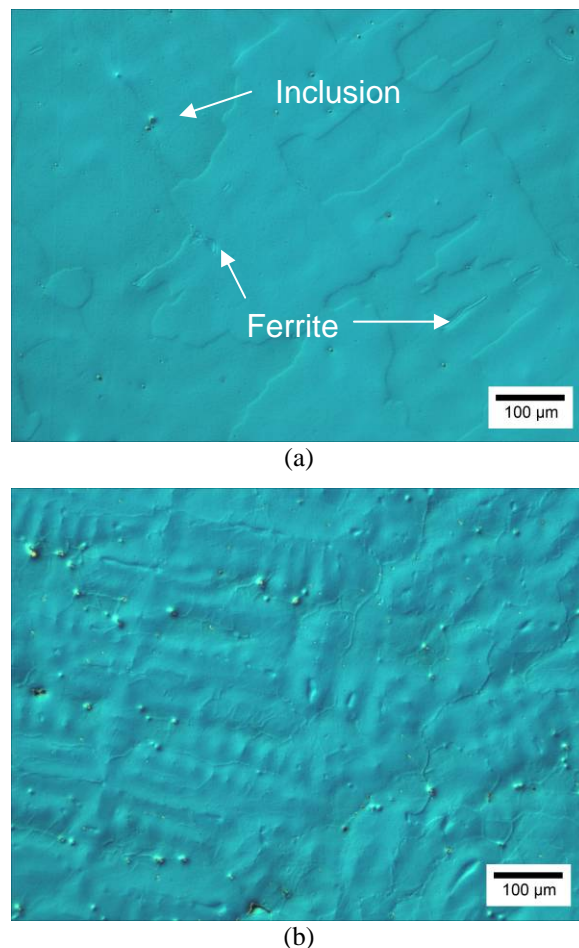

(a)

(b)

Figure 8. Optical micrographs of polished Charpy specimens show a dendritic structure with primary austenite and less than 5% by volume ferrite. The calcium treated plate (a) has a secondary dendrite arm spacing of 81 μm and the non calcium treated plate (b) has a secondary dendrite arm spacing of 42 μm. Inclusion content is more visible in the untreated plate.

The difference in the two steels is directly related to the foundry practice in formulating the steel chemistry. The calcium treatment directly impacts the sulfur content. Calcium is a late addition that reacts in the melt to form a low density sulfide that floats out of the melt. This alloy was also formulated with electrolytic manganese, which is low in phosphorous. The non calcium treated alloy was formulated with ferromanganese, which contains high levels of phosphorus (0.026%). The use of ferromanganese is not a problem in formulating a typical steel, which will have less than 1.5 weight percent manganese. However, these FeMnAlC based materials will contain as much as 30 weight percent manganese

5

and thus ferromanganese should be avoided in producing these lightweight steel alloys.
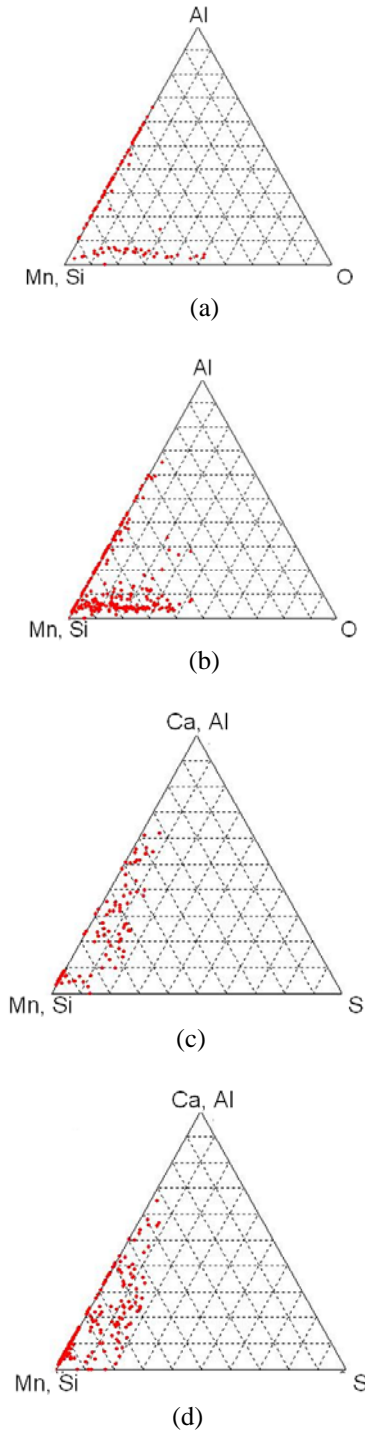

(a)

(b)

(c)

(d)

Figure 9. Chemical mapping of non metallic inclusions for both calcium treated, (a) and (c), and untreated, (b) and (d), FeMnAlC alloys. An equivalent area was scanned on each material and the density of inclusions can be compared using these diagrams. Inclusion chemistries are similar for both steels, but the calcium treated steel has fewer inclusions.

Sulfur (Leslie, 1981), phosphorous (Song et al., 2007), and oxide (Wilson, 1981) content has been shown to decrease Charpy impact energy. The high phosphorous and nonmetallic inclusion content may account for the difference in ballistic performance and Charpy notch toughness. The inclusion concentration shown in Figure 4(c) had chemistries (see Figure 5) that matched those of the Charpy bars (see Figure 9). However, size and quantity comparison of the Charpy bars (see Figure 10) showed the non calcium treated alloy has a larger number of inclusions by a ratio exceeding 2:1. It should be noted that fracture initiation was not limited to inclusion content. Shear band and crack formation were also observed in association with porosity. Thus, proper casting design is also a critical consideration in the ballistic performance of these cast steels.
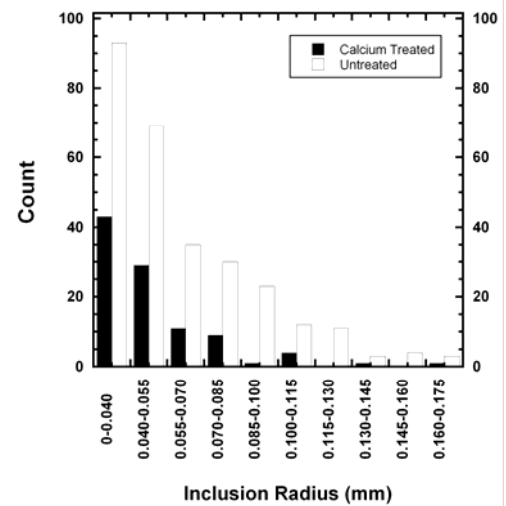

Figure 10. Total inclusion count is plotted by size as measured using the ASPEX-PICA 1020 inclusion analysis software. The calcium treated plate has less than half the number of inclusions of the non calcium treated plate in every size category.

CONCLUSIONS

At equivalent areal densities, FeMnAlC alloys can exceed acceptance criteria of MIL-PRF-32269, and these lightweight steels can achieve greater resistance to the 0.50 caliber FSP than MIL-A46100 alloys. Oxides, sulfides, phosphorous, and porosity are deleterious to both ballistic and Charpy notch toughness of FeMnAlC alloys. Calcium treating the alloy reduced sulfur content and increased ballistic and Charpy impact performance. An increase in the number of inclusions and an increase in phosphorous content accounted for a reduction in 0.30 caliber AP V_{50}, 0.50 caliber FSP V_{50}, and a reduction in Charpy impact properties. Future studies are focused on

improving foundry practices to further reduce defect concentrations in cast FeMnAlC alloys.

ACKNOWLEDGEMENTS

REFERENCES

Frommeyer, G., Brux, U., 2006: Microstructures and Mechanical Properties of High-Strength Fe-Mn-Al-C Light-Weight TRIPLEX Steels, Steel Research Int., 77, 627-633.

Gooch, William A, 1991: US Patent 5007326

Howell, R. A., Lekakh, S. L., Van Aken, D. C., Richards, V. L., 2008: The Affect of Silicon Content on the Fluidity and Microstructure of Fe-Mn-Al-C Alloys, AFS Transactions.

Leslie, W. C., 1981: The Physical Metallurgy of Steels, 300-303.

Song, S. H., Zhuang, H., Wu, J., Weng, L. Q., Yuan, Z. X., Xi, T. H., 2007: Dependence of ductile-to-brittle transition temperature on phosphorous boundary segregation for a 2.25Cr-1Mo Steel, Mat. Sci. and Eng. A., 486, 433-438.

Wilson, A. D., 1981: Comparing the effect of inclusions on ductility, toughness, and fatigue properties, ASTM Through Thickness Tension Testing of Steel Symposium, St. Louis, MO.